High energy resummation of direct photon production at hadronic colliders

Giovanni Diana[1], Juan Rojo[1] and Richard D. Ball[2],

[1] *Dipartimento di Fisica, Università di Milano and INFN, Sezione di Milano,*
Via Celoria 16, I-20133 Milano, Italy
[2] *School of Physics and Astronomy, University of Edinburgh,*
JCMB, KB, Mayfield Rd, Edinburgh EH9 3JZ, Scotland

Abstract:

Direct photon production is an important process at hadron colliders, being relevant both for precision measurement of the gluon density, and as background to Higgs and other new physics searches. Here we explore the implications of recently derived results for high energy resummation of direct photon production for the interpretation of measurements at the Tevatron and the LHC. The effects of resummation are compared to various sources of theoretical uncertainties like PDFs and scale variations. We show how the high–energy resummation procedure stabilizes the logarithmic enhancement of the cross section at high–energy which is present at any fixed order in the perturbative expansion starting at NNLO. The effects of high–energy resummation are found to be negligible at Tevatron, while they enhance the cross section by a few percent for $p_T \lesssim 10$ GeV at the LHC. Our results imply that the discrepancy at small p_T between fixed order NLO and Tevatron data cannot be explained by unresummed high–energy contributions.

arXiv:1006.4250v1 [hep-ph] 22 Jun 2010

The high–energy regime of QCD is the kinematical regime in which hard scattering processes happen at a center-of-mass energy $\sqrt{S}$ which is much larger than the characteristic hard scale of the process Q. An understanding of strong interactions in this region is therefore necessary in order to perform precision physics at high–energy colliders. The high–energy regime is also known as the small-x regime, since it is the regime in which the scaling variable $x = Q^2/S \ll 1$. In this sense, HERA was the first small x machine, while at LHC the small x regime will be even more important.

As is well known, deep–inelastic partonic cross sections and parton splitting functions receive large corrections in the small x limit due to the presence of powers of $\alpha_s \log x$ to all orders in the perturbative expansion [1,2]. This suggests dramatic effects from yet higher orders, so the success of NLO perturbation theory at HERA was for a long time very hard to explain. In the last several years this situation has been clarified [3–9], showing that, once the full resummation procedure accounts for running coupling effects, gluon exchange symmetry and other physical constraints, the effect of the resummation of terms which are enhanced at small x is perceptible but moderate — comparable in size to typical NNLO fixed order corrections in the HERA region.

A major development for high–energy resummation was presented in Ref. [6] where the full small x resummation of deep-inelastic scattering (DIS) anomalous dimensions and coefficient functions was obtained including quarks, which allowed for the first time a consistent small-x resummation of DIS structure functions. Furthermore, the resummation of hard partonic cross sections has been performed for several LHC processes such as heavy quark production [10], Higgs production [11, 12], Drell-Yan [13, 14] and prompt photon production [15]. Hints of the presence of small-x resummation have also recently found in inclusive HERA data [16]. Small–x resummation should also be very important at a high–energy DIS collider like the Large Hadron Electron Collider [17,18]. A more detailed summary of recent theoretical developements in high–energy resummation may be found in Ref. [19]. These results mean that a detailed analysis of the impact of high–energy resummation on precision LHC physics is now possible.

As a part of such a program, in this letter we present a study of the phenomenological implications of the high–energy resummation of direct photon production at hadronic colliders. The production of direct photons [20] is a very important process at hadronic colliders, relevant both for fundamentals reasons (tests of perturbative QCD, measurement of the gluon PDF) and as background to new physics searches, the $H \to \gamma\gamma$ decay being the classical example. In the case of direct photon production, several works have studied in detail the comparison of theoretical QCD predictions with available experimental data from fixed target and collider experiments. Such comparisons have been performed using fixed order NLO computations [21–23], Monte Carlo event generators [24] and supplementing the fixed order result with threshold resummations [25–28]. The latter aim to improve the accuracy of the perturbative prediction in the regime where the photon's p_T is large, close to the kinematic production threshold, where soft gluon emission enhances the cross section.

The present work is instead focused on the low p_T region, where terms of the type $\alpha_s^k \ln^p x$, enhanced by logarithms of the scaling variable $x_\perp \equiv 4p_T^2/S$, are important to all orders in perturbation theory. For this reason we do not consider fixed target data, which are characterized by moderate and large values of $x_\perp$ where high–energy resummation is certainly irrelevant, and concentrate instead on collider data for which the large center of

mass $S \gg p_T^2$ available guarantees that the kinematical region sensitive to small-x effects is explored. As an illustration, if the small-p_T region is defined naively as the region in which the hadronic cross section becomes sensitive to PDFs and partonic coefficient functions for $x \lesssim 10^{-3}$, then at Tevatron this criterion corresponds to $p_T \lesssim 30$ GeV and at the LHC 14 TeV to $p_T \lesssim 200$ GeV.

The prompt photon process is characterized by a hard event involving the production of a single photon. Let us consider the hadronic process

$$H_1(P_1) + H_2(P_2) \to \gamma(q) + X. \tag{1}$$

According to perturbative QCD, the direct and the fragmentation component of the inclusive cross-section at fixed transverse momentum p_T of the photon can be written as [25]

$$p_T^3 \frac{d\sigma_\gamma(x_\perp, p_T^2)}{dp_T} = \sum_{a,b} \int_{x_\perp}^1 dx_1 \, f_{a/H_1}(x_1, \mu_F^2) \int_{x_\perp/x_1}^1 dx_2 \, f_{b/H_2}(x_2, \mu_F^2) \times$$

$$\times \int_0^1 dx \left\{ \delta \left(x - \frac{x_\perp}{x_1 x_2} \right) \mathcal{C}_{ab}^\gamma(x, \alpha_s(\mu^2); p_T^2, \mu_F^2, \mu_f^2) + \right.$$

$$\left. + \sum_c \int_0^1 dz \, z^2 d_{c/\gamma}(z, \mu_f^2) \delta \left(x - \frac{x_\perp}{z x_1 x_2} \right) \mathcal{C}_{ab}^c(x, \alpha_s(\mu^2); p_T^2, \mu_F^2, \mu_f^2) \right\}, \tag{2}$$

where we have introduced the customary scaling variable in terms of the hadronic center-of-mass energy $S = (P_1 + P_2)^2$:

$$x_\perp = \frac{4p_T^2}{S}, \qquad 0 < x_\perp < 1 . \tag{3}$$

The fragmentation component is given in terms of a convolution with the fragmentation function $d_{c/\gamma}(z, \mu_f^2)$. In the factorization formula Eq. (2) we have used the short-distance cross-sections

$$\mathcal{C}_{ab}^{\gamma(c)} \equiv p_T^3 \frac{d\hat\sigma_{ab \to \gamma(c)}(x, \alpha_s(\mu^2); p_T^2, \mu_F^2, \mu_f^2)}{dp_T}, \tag{4}$$

where a, b and c are parton indices (q, $\bar{q}$, g) while $f_{i/H_j}(x_i, \mu_F^2)$ is the parton density at the factorization scale μ_F. The leading order coefficient functions for the Compton scattering channel (qg) and for the quark annihilation channel ($q\bar{q}$) are given by

$$\mathcal{C}_{qg}^{\gamma,\text{LO}}(x) = \frac{\alpha \alpha_s e_q^2 \pi}{2N_c} \frac{x}{\sqrt{1-x}} \left(1 + \frac{x}{4} \right) ,$$

$$\mathcal{C}_{q\bar{q}}^{\gamma,\text{LO}}(x) = \frac{\alpha \alpha_s e_q^2 C_F \pi}{N_c} \frac{x}{\sqrt{1-x}} (2 - x) . \tag{5}$$

In Fig. 1 we show the associated LO Feynman diagrams for these two channels. NLO corrections to the direct partonic cross section in Eq. (2) were computed in Refs. [29–31], while for the fragmentation component they were evaluated in Refs. [32, 33].

The kinematics of direct photon production at hadronic colliders are summarized in Fig. 2, where the minimum value of x, $x_\perp$, probed in the production of a photon with a
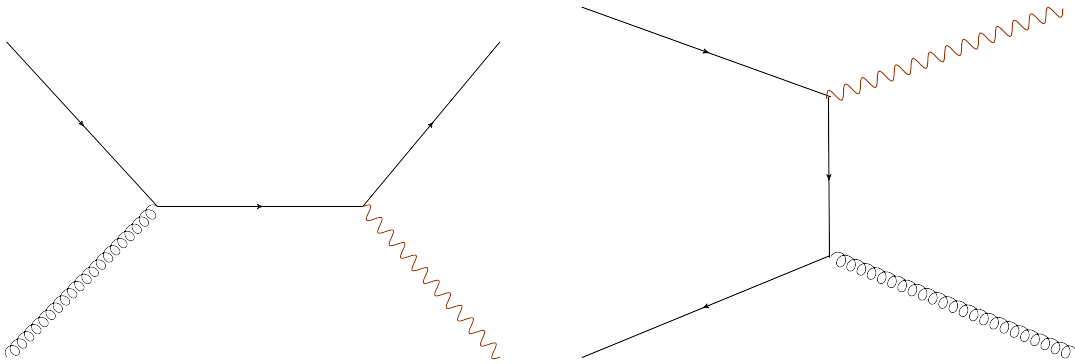
Figure 1: The Feynman diagrams for the direct production of a photon in hadronic collisions at leading order: the gq channel, also known as Compton scattering channel (left) and the $q\bar{q}$ channel, also known as quark annihilation channel (right).

given p_T is shown. For illustrative purposes, the corresponding kinematics for a notional VLHC with $\sqrt{S} = 200$ TeV are also shown. From Fig. 2 follows that collider experiments have the potential reach down to very small values of x, for example, at LHC 14 TeV PDFs and coefficient functions are probed down to $x \sim 10^{-5}$ for a $p_T \sim 20$ GeV photon. This implies that one should worry about those terms in the perturbative expansion which are formally subleading but which are logarithmically enhanced to all orders at small-x, both in the PDF evolution and in the partonic cross-sections.

Due to multiple gluon emissions, the perturbative expansion of the partonic cross sections, Eq. (4), is logarithmically enhanced at small-x starting from NNLO. While at NLO the single gluon emission produces the constant behaviour at low-x of the coefficient function Eq. (4), the NNLO behaves like a single logarithm and, in general, at N^{k}LO, the dominant contribution is given by $\alpha_s(\alpha_s \log x)^{k-1}$.

The high–energy resummed coefficient function of the direct component in Eq. (2) has been obtained in Ref. [15] in the framework of the k_T-factorization theorem, which allows one to perform the leading log resummation in terms of the off shell impact factor, which is the leading order cross section computed with off-shell incoming gluons. Following the resummation procedure one obtains the sum of the leading contributions at high–energy and, by re-expanding in powers of α_s, we have the coefficients of each power of $\log x$ to all orders in perturbation theory.

The high-energy enhanced terms in the direct photon partonic cross section, as discussed in Ref. [15], in N space are given in the qg channel by

$$\tilde{\mathcal{C}}_{qg}^{\gamma}(N, \bar{\alpha}_s, \kappa_r) = \frac{\alpha \alpha_s^2}{N} \sum_{k=0}^{\infty} c_{qg}^{(k)}(\kappa_r) \left(\frac{\bar{\alpha}_s}{N}\right)^{k-1} \tag{6}$$

where the renormalization scale has been set to proportional to the transverse momentum of the photon $\mu_r = \kappa_r p_T$ and where $\bar{\alpha}_s \equiv \alpha_s C_A/\pi$ with α_s is the fixed strong coupling and $\alpha = 1/137$ the electromagnetic coupling constant. The first few coefficients in Eq. (6)
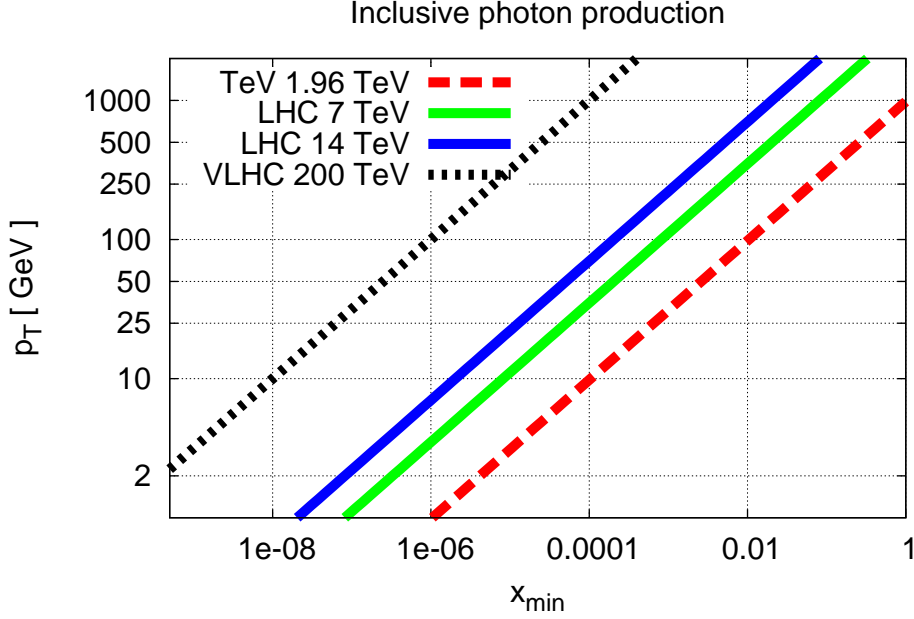
4

Inclusive photon production

Figure 2: The minimum values of x, $x_{\min} = x_\perp = 4p_T^2/S$ which are probed in the production of a direct photon with transverse momentum p_T at hadronic colliders: Tevatron Run II ($\sqrt{S}$=1.96 TeV), LHC 7 TeV and LHC 14 TeV and VLHC 200 TeV. As can be seen from the plot, for the production of a $p_T \sim 20$ GeV photon, PDFs and coefficient functions are probed down to $x \sim 5\,10^{-4}$ at the Tevatron and $x \sim 10^{-5}$ at the LHC 14 TeV. Note that no cuts in rapidity are assumed in the definition of the kinematical ranges, experimentally realistic cuts reduce the reach in x for a given p_T.

read

$$
\begin{aligned}
c_{qg}^{(0)} &= \tfrac{7}{6} \\
c_{qg}^{(1)} &= \tfrac{67}{36} - \tfrac{7}{3}\log\kappa_r \\
c_{qg}^{(2)} &= \tfrac{7}{4}\log^2\kappa_r - \tfrac{29}{9}\log\kappa_r + \tfrac{385}{216} \\
c_{qg}^{(3)} &= -\tfrac{7}{9}\ln^3\kappa_r - \tfrac{55}{26}\ln^2\kappa_r - \tfrac{179}{54}\ln\kappa_r + \tfrac{49}{9}\zeta(3) + \tfrac{2323}{1296}
\end{aligned}
\tag{7}
$$

The NLO term in Eqs. (6-7) gives, in the x-space, the constant value $\alpha\alpha_s^2 67/36$ for $\kappa_r = 1$, in agreement with the fixed order calculation of Refs. [31, 34]. By using the high-energy color charge relation between the hard coefficient functions

$$
\tilde{\mathcal{C}}_{q\bar{q}(q)}^\gamma(N, \alpha_s, \kappa_r) = \frac{C_F}{C_A}\left(\tilde{\mathcal{C}}_{qg}^\gamma(N, \alpha_s, \kappa_r) - \tilde{\mathcal{C}}_{qg}^{\gamma,\mathrm{LO}}(0, \alpha_s, \kappa_r)\right)
\tag{8}
$$

we can obtain the high–energy coefficient function in the $q\bar{q}(q)$ channel.

In the rest of this work we will set $\kappa_r = 1$. In this case, the resummed coefficient function Eq. (6) in $x-$space reads

$$
\begin{aligned}
\mathcal{C}_{qg}^\gamma(x, \bar{\alpha}_s) &= \alpha\alpha_s^2\Big\{ \tfrac{67}{36} + \tfrac{385}{216}\bar{\alpha}_s\ln\tfrac{1}{x} + \tfrac{1}{2}\big(\tfrac{2323}{1296} + \tfrac{49}{9}\zeta(3)\big)\bar{\alpha}_s^2\ln^2\tfrac{1}{x} \\
&\quad + \tfrac{1}{6}\big(\tfrac{14233}{7776} - \tfrac{7}{720}\pi^3 + \tfrac{308}{27}\zeta(3)\big)\bar{\alpha}_s^3\ln^3\tfrac{1}{x} + O(\bar{\alpha}_s^4\ln^4\tfrac{1}{x})\Big\}.
\end{aligned}
\tag{9}
$$

5

Note that the logarithms of x (high–energy enhanced terms) which lead to the rise of the partonic cross section at small-x appear only from NNLO onwards.

However, this formalism is incomplete because it does not account for running coupling effects. Indeed, as shown in Refs. [4, 5, 7, 9] the running of α_s produces a new series of relevant contributions in the high energy limit which modify the nature of the singularity of the anomalous dimension at small-x. At fixed α_s, the resummation procedure requires the identification of the Mellin variable M (conjugate of Q^2) with the sum of the leading singularities of the resummed anomalous dimension

$$M = \gamma_s \left(\alpha_s / N \right). \tag{10}$$

Now, if we include running effects, α_s becomes a function of Q^2 which corresponds to an operator in M-Mellin space and Eq. (10) is understood as an equality between operators. At the running coupling level, the identification given by Eq. (10) produces a class of terms proportional to increasing derivatives of γ_s. In practice these are most easily computed by using Eq. (10) to turn the expansion Eq. (6) in powers of $\bar{\alpha}_s / N$ into an expansion in powers of M: since powers of m correspond to derivatives with respect to $\ln Q^2$, this then gives the resummed coefficient function even when the coupling runs. For a thorough description of the inclusion of running coupling effects see Refs. [5, 6].

In this way a fully resummed coefficient function in the $\overline{\text{MS}}$ scheme, which can be consistently matched to standard $\overline{\text{MS}}$ fixed order computations, can be obtained. This resummed coefficient function $\mathcal{C}_{ab}^{\gamma,\text{res}}$ can be matched to the fixed order NLO coefficient function to obtain a resummed coefficient functions which reproduces at large-x the fixed order result,

$$\mathcal{C}_{ab}^{\gamma,\text{NLOres}} = \mathcal{C}_{ab}^{\gamma,\text{NLO}} + \mathcal{C}_{ab}^{\gamma,\text{res}} - \mathcal{C}_{ab}^{\gamma,\text{dc}} . \tag{11}$$

In Eq. (11) the matching between the fixed order NLO result and the resummed one has been performed being careful of avoiding double counting. Therefore, the double counting contribution $\mathcal{C}_{ab}^{\gamma,\text{dc}}$, that is, the terms in Eq. (9) up to $\mathcal{O}\left(\alpha \alpha_s^2\right)$ is removed from the NLO coefficient functions. The fixed order NLO coefficient functions are taken from Ref. [31].

Note that Eq. (11) accounts for the high–energy resummation of the direct part of the photon production cross section without photon isolation effects. At the resummed level, the effects of the photon isolation in the coefficient function Eq. (6) can be computed in the small cone approximation. It can be shown that isolation leads an effect analogous to the variation of the renormalization scale, that is, using the usual isolation with a cone of radius R implies a modifications of the renormalization scale $\kappa_r \to \kappa_r R$. Note also that we do not attempt a resummation of the fragmentation component of the photon production cross section, which in any case is very much suppressed by the photon isolation.

In Fig. 3 we show the LO, NLO and resummed coefficient functions for the two relevant channels: Compton scattering, qg, and quark annihilation, $q\bar{q}$. On top of these, we also show the NLO coefficient functions supplemented by the NNLO high–energy contribution (the $\mathcal{O}\left(\alpha \alpha_s^3\right)$ term in Eq. (9)), and similarly for NLO plus NNNLO high–energy contributions (the $\mathcal{O}\left(\alpha \alpha_3^3\right)$ and $\mathcal{O}\left(\alpha \alpha_s^4\right)$ terms in Eq. (9). These two latter cases are shown for illustration, with the well know caveat that subleading corrections at a fixed α_s might sizably reduce the effect of the leading high–energy contributions. Fig. 3 shows the important result that the steep rise at small-x of the fixed order coefficient function due to the increasing powers of $\log x$ is stabilized after the including the running coupling effects, as happens for DIS [6].
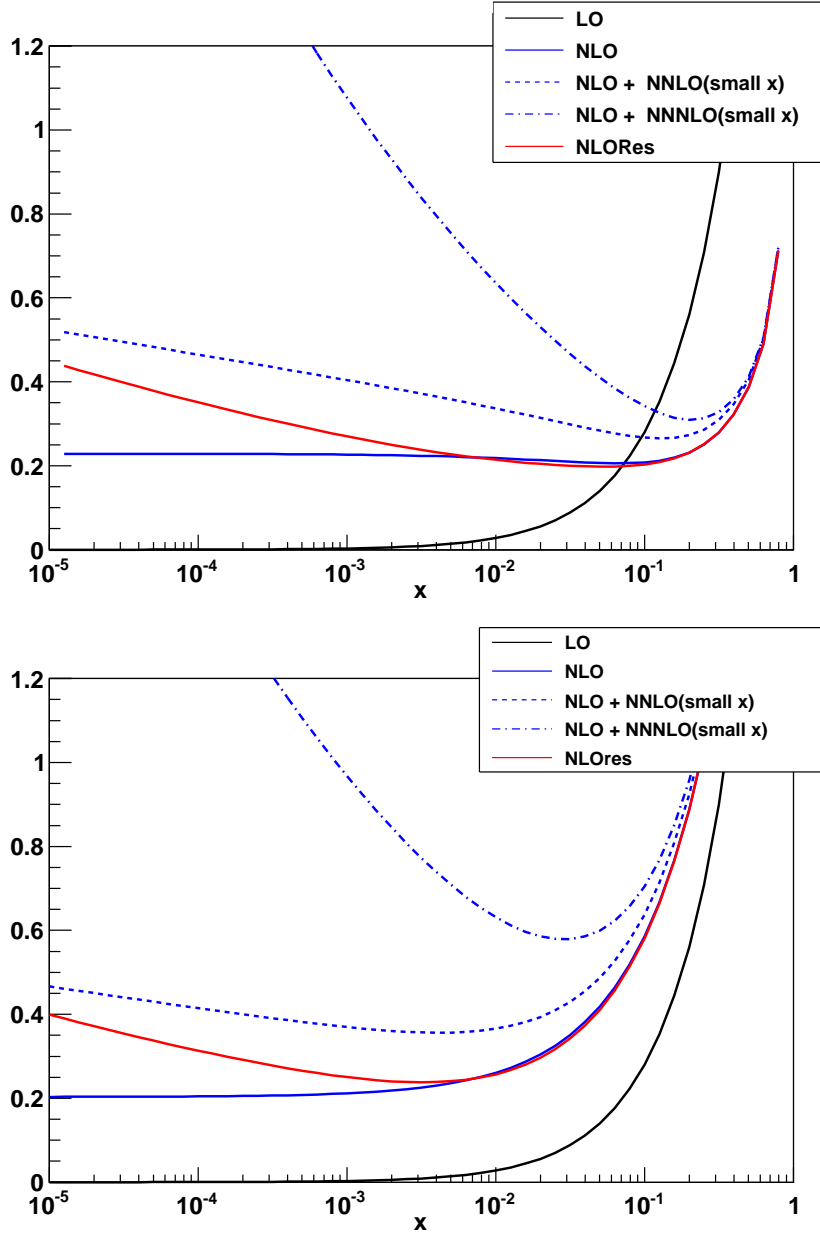
Figure 3: Upper plot: the coefficient functions (partonic cross sections) for direct photon production in the qg (Compton) channel. The following approximations to the partonic cross section are shown: LO (black, solid), NLO (blue, solid), NLO with the addition of the dominant small-x NNLO terms (blue, dashed), NLO with the addition of the dominant small-x NNNLO terms (blue, dot-dashed), and finally the high–energy resummed coefficient function, suitably matched of the fixed order NLO Eq. (11) (red, solid). Lower plot: the same comparison for the coefficient functions in the $q\bar{q}$ (quark annihilation) channel. Note that the coefficient functions rise at small-x begins at NNLO only.

Now that the resummed partonic cross-section, suitably matched to the fixed-order NLO result, has been obtained, we can use it to estimate the impact of high–energy resummation on the hadronic cross–section, Eq. (2), at the Tevatron and at the LHC. The fixed order NLO computation of isolated photon production has been obtained using the code of Ref. [31]. The small cone approximation for the isolation criterion has been used, which is shown to be an excellent approximation [35] to the exact result for typical isolation parameters. The photon fragmentation functions are the BFG set [36], although the choice is irrelevant since the fragmentation component is severely suppressed by the isolation criterion.

Note that in the following the same PDF set will be used used both in the NLO and in the resummed computations. The motivation for this is that we are interested only in the impact of the resummation of the partonic cross-section. A consistent high–energy resummed cross section would require PDFs obtained from a global analysis based on small-x resummation, which are not available yet.

In order to assess the impact of high–energy resummation at the Tevatron, we consider recent Run II data on isolated photon production from the CDF collaboration [37]. CDF data is provided in the range $30 \,\mathrm{GeV} \leq \mathrm{p_T} \leq 350 \,\mathrm{GeV}$, integrated in the photon's rapidity range $|\eta^\gamma| \leq 1.0$. The parameters of the photon isolation criterion in the theoretical calculation match those of the experimental analysis, namely $R = 0.4$ and $E_T^{\mathrm{had}} \leq 2 \,\mathrm{GeV}$. The parton distribution set used for the comparison with experimental data is the recent NNPDF2.0 global analysis [38]. As compared to previous NNPDF sets [39–42], NNPDF2.0 has a more precise gluon both at small-x from the combined HERA-I dataset and at large-x from the Tevatron inclusive jet data, which translate into very accurate predictions for direct photon production.

In Fig. 4 we present the results of this comparison between the fixed order NLO and the resummed predictions with the recent direct photon measurements from the CDF Collaboration at Run II. We show as well the PDF uncertainties and the theoretical uncertainties from missing higher orders estimated as usual varying the scales of the NLO expressions. Good agreement between NLO QCD and experimental data within the experimental uncertainties is found through most of the p_T range, except for a systematic discrepancy at small p_T. This discrepancy is present also for other PDF sets [23] as well as for the D0 data [43].

Since the high–energy resummed coefficient functions, Fig. 3 are integrated in the photon's rapidity η^γ, we will assume that the effects of the resummation are constant in η^γ. This means that the resummed result in Fig. 4 has been obtained as follows

$$\frac{d\sigma_\gamma^{\mathrm{res}}\left(x_\perp, p_T^2, |\eta^\gamma| \leq \eta_{\mathrm{cut}}\right)}{dp_T} = \frac{d\sigma_\gamma^{\mathrm{NLO}}\left(x_\perp, p_T^2, |\eta^\gamma| \leq \eta_{\mathrm{cut}}\right)}{dp_T} \frac{d\sigma_\gamma^{\mathrm{res}}\left(x_\perp, p_T^2\right)}{d\sigma_\gamma^{\mathrm{NLO}}\left(x_\perp, p_T^2\right)} \qquad (12)$$

This approximation could be improved by computing the high–energy resummation of the photon rapidity distribution, for which qualitative arguments suggest that the impact of resummation is more important towards forward rapidities.

To estimate the theoretical uncertainty due to missing higher orders terms in the NLO computation the common scale $\kappa_r = \kappa_F = \kappa_f$ has been varied within a reasonable range. In particular we have computed the cross section for $\kappa_r = 0.5$, 1 and 2. The scale variation uncertainty is defined as the envelope of the most extreme results obtained this way for any given p_T. As seen in Fig. 4, PDF uncertainties for isolated photon production at the

Tevatron are below 5% in all the p_T range, and $\mathcal{O}(2\%)$ in the small $p_T \lesssim 100$ GeV region. Scale variation uncertainties are $\mathcal{O}(5\%)$ approximately constant in p_T.

We do not attempt here to estimate the combined PDF and α_s uncertainty [44–46], which could be important in direct photon production since the cross section starts at $\mathcal{O}(\alpha\alpha_s)$. Moreover, in this work we do not address the important issue of the compatibility of predictions obtained from different modern PDF sets, which has already been presented in detail in Ref. [23].

From Fig. 4 it is clear that at the Tevatron the prediction from high–energy resummation is essentially identical to that of the fixed order NLO computation. This might seem unintuitive, since we have shown in Fig. 3 that the respective coefficient functions are rather different in the small x region within the kinematical reach of experimental data (Fig. 2). In order to explain this result, let us define the contribution to the total cross section for $x \geq x_\perp^{\min}$ as follows

$$
\mathbf{q}^3 \frac{d\sigma_\gamma(x_\perp, x_\perp^{\min}, p_T^2)}{d\mathbf{q}} \equiv \sum_{a,b} \int_{x_\perp^{\min}}^1 dx_1\, f_{a/H_1}(x_1, \mu_\mathrm{F}^2) \int_{x_\perp^{\min}/x_1}^1 dx_2\, f_{b/H_2}(x_2, \mu_\mathrm{F}^2) \times
$$
$$
\times \int_0^1 dx \left\{ \delta\left(x - \frac{x_\perp}{x_1 x_2} \right) \mathcal{C}_{ab}^\gamma(x, \alpha_s(\mu^2); p_T^2, \mu_\mathrm{F}^2, \mu_\mathrm{f}^2) + \text{fragmentation} \right\} \tag{13}
$$

and then we can construct the ratio

$$
R_\gamma\left(x_\perp, x_\perp^{\min}, p_T^2\right) \equiv \frac{d\sigma_\gamma(x_\perp, x_\perp^{\min}, p_T^2)/dp_T}{d\sigma_\gamma(x_\perp, x_\perp, p_T^2)/dp_T} \tag{14}
$$

which measures the fraction of the cross–section for which PDFs and coefficient functions with $x \geq x_\perp^{\min}$ are probed.

In Fig. 5 we show this ratio at the Tevatron, the LHC and the notional VLHC for the production of a photon with $p_T = 20$ GeV. We observe that the direct photon cross section at the Tevatron is completely dominated by the region $x \gtrsim 5\,10^{-2}$. In this region, the resummed coefficient functions are almost identical to the fixed order NLO ones. Therefore, despite the fact that the values of x probed in small-p_T photon production are such that the resummed coefficient functions, Fig. 3, differ sizably from their fixed order NLO counterparts, this difference is restricted to a region with very little weight in the total cross–section. This feature of direct photon production (shared also by Higgs production [11, 12]) explains the smallness of high–energy resummation at the Tevatron. Note that this applies to the rapidity integrated cross–section, it is conceivable that more important effects are observed if one is restricted to forwards rapidities.

Note that Fig. 5 implies also that direct photon production is sensitive to the large-x PDFs, especially the gluon, but not to the small-x ones: the inclusion of collider direct photon data into a global PDF analysis might improve the precision of the gluon at large-x, but not at small-x.

Let us finish the discussion on the impact of high-energy resummation at the Tevatron by noting that the origin of the discrepancy between NLO QCD and experimental data at small p_T is still not completely understood, in particular, it is not caused by unresummed terms in the high-energy regime. However, as we have discussed, since the direct photon cross section is much more sensitive to large-x effects, this discrepancy could be partially cured by soft resummation [28].
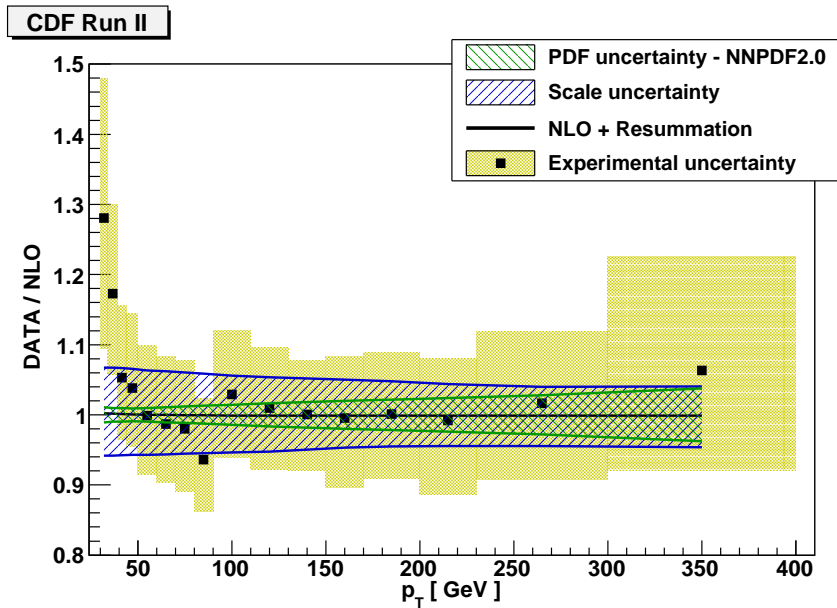
Figure 4: Comparison between the NLO cross section and the recent CDF data using the NNPDF2.0 PDF set. The solid black line is the ratio between the high–energy resummed result and the NLO prediction, as can be seen, the two results are essentially identical. The scale variation uncertainty corresponds to the NLO calculation.

Now we turn to discuss the phenomenological impact of the resummation at LHC. At the LHC, the production cross section of isolated photons is much larger than at the Tevatron, which will make possible a high-statistics measurement. The ALICE, ATLAS, CMS and LHCb experiments at the LHC have photon reconstruction capabilities with the electromagnetic calorimetry in various rapidity ranges [23]. The two main LHC experiments can measure photons in the central rapidity region $|\eta^\gamma| \lesssim 3$ down to $p_T = 10$ GeV, ALICE can do measurements in the central region $|\eta^\gamma| \lesssim 0.7$ down to $p_T = 5$ GeV, while LHCb can measure forwards photons, $2 \leq |\eta^\gamma| \leq 5$ in the low $p_T \leq 20$ GeV region as well. The LHCb measurements are specially interesting since small-x resummation effects, which are only important at low p_T, should be enhanced at forward rapidities.

From the discussion in the case of the Tevatron, we expect the impact of high–energy resummation to be also small at the LHC. To illustrate such impact, in Fig. 6 we show the ratio between the resummed and NLO direct photon production cross section at LHC, for $\sqrt{S} = 14$ TeV. We show for simplicity the direct part of the photon production cross section only. No cuts in the photon's rapidity are imposed. We have used again the NNPDF2.0 set for the theoretical prediction, and scale variation uncertainty is estimated as discussed above.

From Fig. 6 we observe that the effect of high–energy resummation is very small above $p_T \sim 10$ GeV, and it is only for photon transverse momenta in the range 2 GeV $\lesssim$ p$_T$ $\lesssim$ 10 GeV that it becomes of the order of a few percent. The origin of the smallness of the high–energy resummation can be traced back, as in the case of the Tevatron to Fig. 5: the direct photon cross section for the production of a photon with $p_T = 20$ GeV is completely
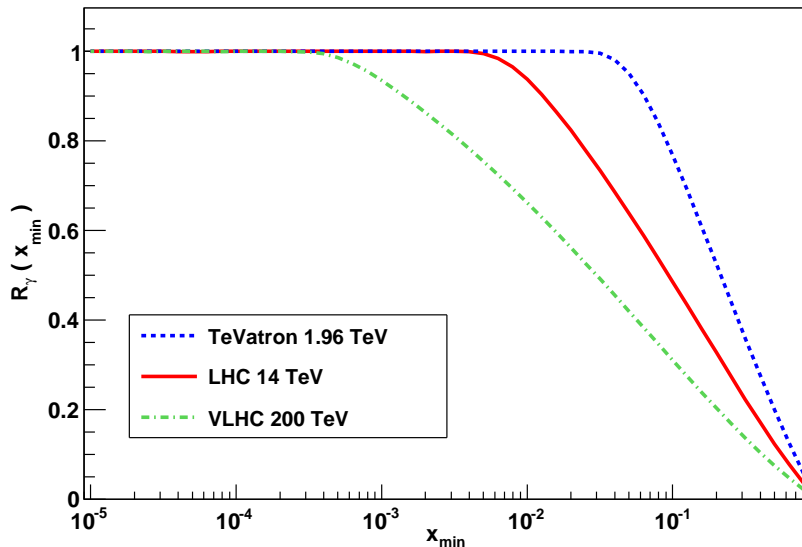
10

Figure 5: The ratio R_γ, Eq. (13), as a function of $x_\perp^{\min}$ at the LHC $\sqrt{S} = 14$ TeV (red solid line) and at Tevatron Run II $\sqrt{S} = 1.96$ TeV (blue dashed line) for the production of photon with $p_T = 20$ GeV. It is clear that the cross-section is dominated by the contribution of the coefficient function at medium and large-x, $x \gtrsim 5\,10^{-3}$ for LHC and $x \gtrsim 5\,10^{-2}$ for the Tevatron. The fact that the total cross section is insensitive to the partonic cross-sections at small-x explains the reduced impact of the high–energy resummation at hadronic colliders.

dominated by the region $x \gtrsim 5\,10^{-3}$. In this region, the resummed coefficient functions are almost identical to the fixed order NLO ones. It is only for smaller values of p_T that the difference between NLO and resummed coefficient functions at small-x, evident from Fig. 3, begin to contribute to the total cross section. At very small-p_T the effects of high–energy resummation are much smaller than the PDF uncertainties. This implies that the small-p_T region can be used to constrain accurately the gluon PDF, provided that systematic experimental uncertainties in this region can be kept under control.

Let us emphasize however that the smallness of the high–energy resummation with respect to fixed order NLO does not imply that resumming high–energy enhanced terms is not relevant at hadronic colliders. Indeed, the crucial role of high–energy resummation is to cure the instability of the cross section which appears in any fixed order calculation at high–energy starting from NNLO. To illustrate this point, in Fig. 6 we also show the results for direct photon production if the dominant NNLO contribution at small-x (the term proportional to $\mathcal{O}\left(\alpha_s^3\right)$ in Eq. (9) is added to the fixed order NLO result, as an approximation to the full fixed order NNLO result. We see that here the difference with respect NLO is more important, being $\sim 10\%$ at $p_T \sim 20$ GeV and much larger at even smaller p_T. The corresponding effect would be even larger for the dominant NNNLO corrections. Thus the full high-energy resummation is required in order to obtain stable predictions for future higher order calculations of direct photon production (starting from NNLO accuracy) at small p_T at hadronic colliders.
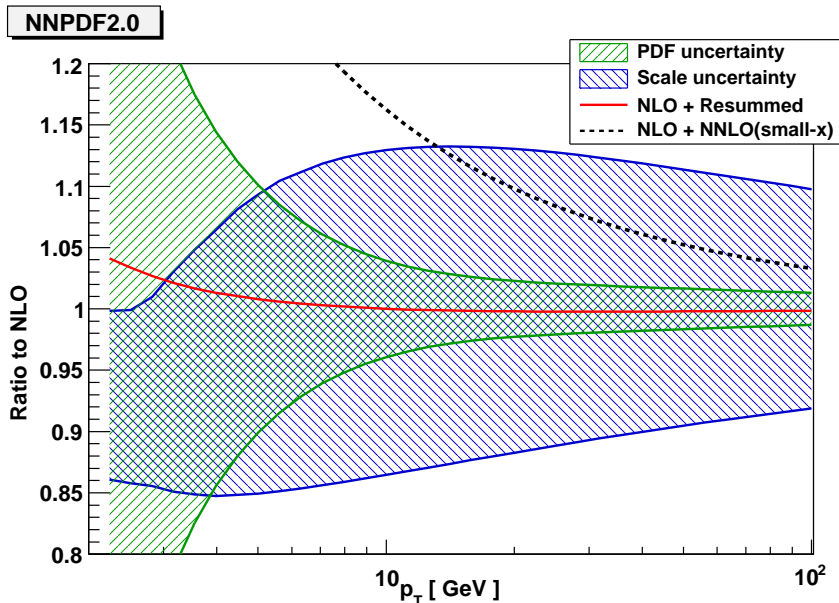
Figure 6: Ratio between resummed and NLO prediction (solid red line) for the inclusive cross section at LHC, for a center of mass energy of $\sqrt{S} = 14$ TeV. The NNPDF2.0 set has been used to compute the theoretical prediction. PDF and scale variation uncertainties are also shown. We also show the ratio to NLO of the approximated NNLO result, where the dominant NNLO contributions at small x have been added to the fixed order NLO result (black dashed line) .

Finally, in Fig. 7 we show the impact of the resummation of the high–energy coefficient function for photon production at a notional VLHC with $\sqrt{S} = 200$ TeV. From Fig. 5 we see that for a 20 GeV photon the cross section is sensitive to the coefficient functions with $x \geq 5\,10^{-4}$, so one expected the effects of the resummation to be more important that at lower CM energies. However, even at this huge energy, the effect is of a few percent at most at the smallest p_T.

To summarize, in this letter results for the high energy resummation of direct photon production have been matched to NLO computations and predictions for hadronic colliders have been obtained. We have shown that main impact of the full high–energy resummation procedure is to stabilize the logarithmic enhancement of the cross section at high energies which is present at any fixed order in the perturbative expansion starting at NNLO. At the Tevatron the effects of the resummation are completely negligible, while at the LHC high–energy resummation of the partonic cross section enhances the hadronic cross section be a few percent at small p_T, $p_T \lesssim 10$ GeV. One important implication of our results is that the small p_T discrepancy between NLO QCD and Tevatron data cannot be described by unresummed higher order contributions enhanced in the high–energy regime. We have also shown that at the LHC the full resummation of the inclusive direct photo cross-section is very close to the fixed order NLO QCD result, becoming significant only at very low p_T, and that even at a VLHC resummation effects are rather small in this channel.
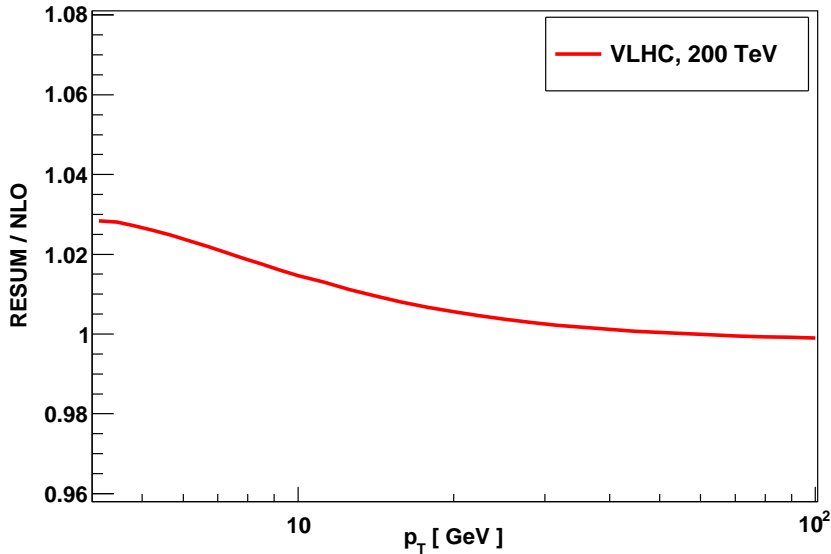
12

Figure 7: Ratio between resummed and NLO prediction (solid red line) for the cross section for photon production, integrated in rapidity, at a notional VLHC with a center of mass energy of $\sqrt{S} = 200$ TeV. The NNPDF2.0 set has been used to compute the theoretical prediction. Note that the very large PDF and scale variation uncertainties are not shown for simplicity.

References

[1] S. Catani, M. Ciafaloni and F. Hautmann, Nucl. Phys. B366 (1991) 135.

[2] S. Catani and F. Hautmann, Nucl. Phys. B427 (1994) 475, hep-ph/9405388.

[3] G. Altarelli, R.D. Ball and S. Forte, Nucl. Phys. B674 (2003) 459, hep-ph/0306156.

[4] G. Altarelli, R.D. Ball and S. Forte, Nucl. Phys. B742 (2006) 1, hep-ph/0512237.

[5] R.D. Ball, Nucl. Phys. B796 (2008) 137, 0708.1277.

[6] G. Altarelli, R.D. Ball and S. Forte, Nucl. Phys. B799 (2008) 199, 0802.0032.

[7] M. Ciafaloni et al., Phys. Rev. D68 (2003) 114003, hep-ph/0307188.

[8] M. Ciafaloni et al., Phys. Lett. B587 (2004) 87, hep-ph/0311325.

[9] M. Ciafaloni et al., JHEP 08 (2007) 046, 0707.1453.

[10] R.D. Ball and R.K. Ellis, JHEP 05 (2001) 053, hep-ph/0101199.

[11] S. Marzani et al., Nucl. Phys. B800 (2008) 127, 0801.2544.

[12] S. Marzani et al., Nucl. Phys. Proc. Suppl. 186 (2009) 98, 0809.4934.

[13] S. Marzani and R.D. Ball, Nucl. Phys. B814 (2009) 246, 0812.3602.

[14] S. Marzani and R.D. Ball, (2009), 0906.4729.

[15] G. Diana, Nucl. Phys. B824 (2010) 154, 0906.4159.

[16] F. Caola, S. Forte and J. Rojo, Phys. Lett. B686 (2010) 127, 0910.3143.

[17] J. Rojo et al., (2009), 0907.0443.

[18] J. Rojo and F. Caola, (2009), 0906.2079.

[19] S. Forte, G. Altarelli and R.D. Ball, Nucl. Phys. Proc. Suppl. 191 (2009) 64, 0901.1294.

[20] J.F. Owens, Rev. Mod. Phys. 59 (1987) 465.

[21] J. Huston et al., Phys. Rev. D51 (1995) 6139, hep-ph/9501230.

[22] P. Aurenche et al., Phys. Rev. D73 (2006) 094007, hep-ph/0602133.

[23] R. Ichou and D. d'Enterria, (2010), 1005.4529.

[24] S. Hoeche, S. Schumann and F. Siegert, Phys. Rev. D81 (2010) 034026, 0912.3501.

[25] S. Catani et al., JHEP 03 (1999) 025, hep-ph/9903436.

[26] N. Kidonakis and J.F. Owens, Phys. Rev. D61 (2000) 094004, hep-ph/9912388.

[27] P. Bolzoni, S. Forte and G. Ridolfi, Nucl. Phys. B731 (2005) 85, hep-ph/0504115.

[28] T. Becher and M.D. Schwartz, (2009), 0911.0681.

[29] P. Aurenche et al., Phys. Lett. B140 (1984) 87.

[30] P. Aurenche et al., Nucl. Phys.. B297 (1988) 661.

[31] L.E. Gordon and W. Vogelsang, Phys. Rev. D48 (1993) 3136.

[32] F. Aversa et al., Nucl. Phys. B327 (1989) 105.

[33] P. Aurenche et al., Nucl. Phys. B399 (1993) 34.

[34] R.K. Ellis and D.A. Ross, Nucl. Phys. B345 (1990) 79.

[35] S. Catani et al., JHEP 05 (2002) 028, hep-ph/0204023.

[36] L. Bourhis, M. Fontannaz and J. Guillet, Eur. Phys. J. C2 (1998) 529.

[37] The CDF Collaboration, .T. Aaltonen, (2009), 0910.3623.

[38] The NNPDF Collaboration, R.D. Ball et al., (2010), Nucl. Phys. B in press, 1002.4407.

[39] The NNPDF Collaboration, L. Del Debbio et al., JHEP 03 (2007) 039, hep-ph/0701127.

[40] The NNPDF Collaboration, R.D. Ball et al., Nucl. Phys. B809 (2009) 1, 0808.1231.

[41] The NNPDF Collaboration, R.D. Ball et al., Nucl. Phys. B823 (2009) 195, 0906.1958.

[42] The NNPDF Collaboration, R.D. Ball et al., JHEP 05 (2010) 075, 0912.2276.

[43] The D0 Collaboration, V.M. Abazov et al., Phys. Lett. B639 (2006) 151, hep-ex/0511054.

[44] F. Demartin et al., (2010), 1004.0962.

[45] A.D. Martin et al., Eur. Phys. J. C64 (2009) 653, 0905.3531.

[46] H.L. Lai et al., (2010), 1004.4624.